Letters

A Fixed-Length Transfer Delay Based Adaptive Frequency-Locked Loop for Single-Phase Systems

Zhiyong Dai, Zhen Zhang, Yongheng Yang, *Senior Member, IEEE*, Frede Blaabjerg, *Fellow, IEEE*, Yigeng Huangfu, *Senior Member, IEEE*, and Juxiang Zhang

***Abstract*—This letter presents an adaptive frequency-locked loop (FLL) with fixed-length transfer delay units for single-phase systems. By analyzing the relationship between the grid voltage and its transfer delay signals, a linear regression model of the grid voltage is established. Accordingly, a transfer delay based adaptive FLL (TD-AFLL) is proposed. A mathematic proof indicates that the proposed TD-AFLL can reject both phase offset errors and double-frequency oscillatory errors. Thus, the grid voltage parameters can be estimated accurately, even when the frequency drifts away from its nominal value. Moreover, fast dynamics of the TD-AFLL are achieved due to the transfer delay structure. Experiments verify the effectiveness of the proposed method.**

***Index Terms*—Fixed-length transfer delay, frequency-locked loop (FLL), frequency variations, grid synchronization, single-phase systems.**

I. Introduction

IN THE past decades, single-phase inverters for vehicle-to-grid/grid-to-vehicle devices and small-scale photovoltaic systems have been extensively developed. In grid-connected applications, the grid current has to be synchronized with the grid voltage. The grid synchronization typically estimates the frequency, amplitude, and phase angle of the grid voltage [1]. To achieve so, many methods are proposed in the literature. Among those, phase-locked loops (PLLs) are one of the favorites [2]–[6]. For instance, the transfer delay based PLL (TD-PLL), inverse-park transformation based PLL, generalized integrator

Manuscript received July 5, 2018; revised July 22, 2018 and August 20, 2018; accepted September 8, 2018. Date of publication September 18, 2018; date of current version March 29, 2019. This work was supported in part by the National Young Natural Science Foundation of China under Grant 51707140, in part by the Natural Science Basic Research Plan in Shaanxi Province of China under Grant 2018JQ5061, and in part by the Fundamental Research Funds for Central Universities under Grants JBX170416 and XJS17037. *(Corresponding author: Zhen Zhang.)*

Z. Dai and J. Zhang are with the School of Mechanical and Electrical Engineering, Xidian University, Xi'an 710071, China (e-mail:

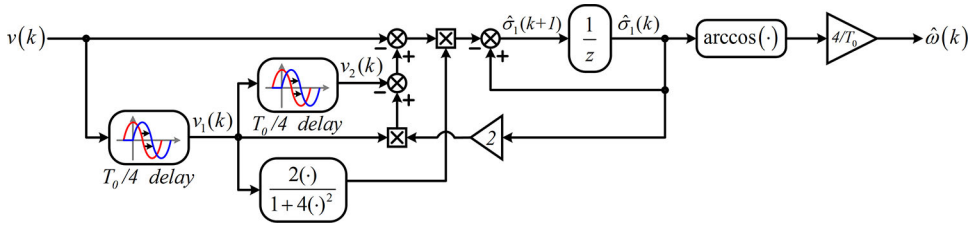

Fig. 1. Structure of the proposed transfer delay based adaptive frequency-locked loop (TD-AFLL).

II. Linear Regression Model of the Grid Voltage

In single-phase systems, the grid voltage can be given as

$$v(t) = V\sin(\omega t + \phi) = V\sin\psi \tag{1}$$

where ω, V, and ψ are the frequency, amplitude, and phase angle of the grid voltage, respectively. Discretizing the grid voltage with the sample time T_s yields

$$v(k) = V\sin(\omega k T_s + \phi), \quad k = 0, 1, 2, \ldots \tag{2}$$

Similar to the prior-art TD-PLLs, two transfer delay units are applied to the discretized grid voltage $v(k)$. They can be expressed as

$$v_1(k) = v\left(k - \frac{T_0}{4T_s}\right) = V\sin\left(\omega k T_s - \frac{\omega T_0}{4} + \phi\right) \tag{3}$$

$$v_2(k) = v\left(k - \frac{T_0}{2T_s}\right) = V\sin\left(\omega k T_s - \frac{\omega T_0}{2} + \phi\right) \tag{4}$$

in which $k = 0, 1, 2, \ldots$ and T_0 is the nominal period of the grid voltage. Equations (3) and (4) can be further expressed as

$$v_1(k) = \sigma_1 V\sin(\omega k T_s + \phi) - \sigma_2 V\cos(\omega k T_s + \phi) \tag{5}$$

$$v_2(k) = \sigma_3 V\sin(\omega k T_s + \phi) - \sigma_4 V\cos(\omega k T_s + \phi) \tag{6}$$

where $\sigma_1, \sigma_2, \sigma_3, \sigma_4$ are coefficients that can be calculated by

$$\sigma_1 = \cos\frac{\omega T_0}{4}, \ \sigma_2 = \sin\frac{\omega T_0}{4} \tag{7}$$

$$\sigma_3 = \cos\frac{\omega T_0}{2}, \ \sigma_4 = \sin\frac{\omega T_0}{2} \tag{8}$$

and furthermore

$$\sigma_3 = 2\sigma_1^2 - 1, \ \sigma_4 = 2\sigma_1\sigma_2. \tag{9}$$

Since $0 < \omega T_0/4 < \pi$, the following holds:

$$\sigma_2 \neq 0. \tag{10}$$

Substituting (2) into (5) and (6) gives

$$\sigma_2 V\cos(\omega k T_s + \phi) = \sigma_1 v(k) - v_1(k) \tag{11}$$

$$\sigma_4 V\cos(\omega k T_s + \phi) = \sigma_3 v(k) - v_2(k). \tag{12}$$

According to (7)–(12), it can be obtained that

$$v(k) + v_2(k) = 2\sigma_1 v_1(k). \tag{13}$$

Equation (13) is the linear regression model of the grid voltage $v(k)$, which describes the relationship among the grid voltage and its transfer delay signals. Clearly, in (13), $v(k)$ is measurable, $v_1(k)$ and $v_2(k)$ are available through the transfer delay blocks, and σ_1 is the unknown parameter related to the grid frequency ω. Obviously, once σ_1 is estimated accurately, the grid voltage frequency ω can be calculated, i.e., the synchronization is achieved. With σ_1 and ω, the amplitude and phase angle can be obtained [e.g., following (23)–(25)].

III. Proposed TD-AFLL Algorithm

In this section, based on the linear model (13), the TD-AFLL is proposed to estimate the unknown parameter σ_1 and the grid voltage frequency ω, and then the amplitude and phase angle are also obtained accurately. First, the TD-AFLL is designed as

$$\hat{\sigma}_1(k+1) = \hat{\sigma}_1(k) - \frac{2v_1(k)}{1+4v_1^2(k)}(2\hat{\sigma}_1(k)v_1(k) - v(k) - v_2(k)) \tag{14}$$

$$\hat{\omega}(k) = \frac{4\arccos(\hat{\sigma}_1(k))}{T_0} \tag{15}$$

where $\hat{\sigma}_1(k)$ and $\hat{\omega}(k)$ are the estimates of σ_1 and ω, respectively. Subsequently, the structure of the TD-AFLL is shown in Fig. 1. Next, a strict derivation is provided to prove that (14) and (15) are an FLL, and the TD-AFLL estimates the grid frequency with zero steady-state errors.

First, consider the estimation error as

$$\tilde{\sigma}_1(k) = \hat{\sigma}_1(k) - \sigma_1. \tag{16}$$

Then, according to (13)–(16), it is derived that

$$\begin{aligned}\tilde{\sigma}_1(k+1) &= \hat{\sigma}_1(k+1) - \sigma_1 \\ &= \hat{\sigma}_1(k) - \sigma_1 - \frac{2v_1(k)}{1+4v_1^2(k)}(2\hat{\sigma}_1(k)v_1(k) \\ &\quad - v(k) - v_2(k)) \\ &= \tilde{\sigma}_1(k) - \frac{2v_1(k)}{1+4v_1^2(k)}(2\hat{\sigma}_1(k)v_1(k) - 2\sigma_1 v_1(k)) \\ &= \tilde{\sigma}_1(k) - \frac{4v_1^2(k)}{1+4v_1^2(k)}\tilde{\sigma}_1(k) \\ &= \frac{1}{1+4v_1^2(k)}\tilde{\sigma}_1(k).\end{aligned} \tag{17}$$

Iterating (17) yields

$$\begin{aligned}\tilde{\sigma}_1(k) &= \frac{1}{1+4v_1^2(k-1)}\tilde{\sigma}_1(k-1)\\ &= \frac{1}{1+4v_1^2(k-1)}\frac{1}{1+4v_1^2(k-2)}\tilde{\sigma}_1(k-2)=\cdots\\ &= \frac{1}{1+4v_1^2(k-1)}\frac{1}{1+4v_1^2(k-2)}\cdots\frac{1}{1+4v_1^2(0)}\tilde{\sigma}_1(0)\end{aligned} \tag{18}$$

where $\tilde{\sigma}_1(0)$ is the initial estimation error and $v_1(0)$ is the initial transfer delay voltage of v_1.

For convenience, it is assumed that there are m nonzeros in $\{v_1(0), v_1(1), \ldots, v_1(k-1)\}$ and these are referred as $v_1(i_1), v_1(i_2), \ldots, v_1(i_m)$. Among the nonzero elements, the minimum is denoted as $v_{1\min}(i)$.

Obviously, when $v_1(j)=0$ with $j \in \{0,1,\ldots,k-1\}$, $1/(1+4v^2{}_1(j))=1$. With the above-mentioned assumption, $\tilde{\sigma}_1(k)$ is rewritten as

$$\tilde{\sigma}_1(k) = \frac{1}{1+4v_1^2(i_1)}\frac{1}{1+4v_1^2(i_2)}\cdots\frac{1}{1+4v_1^2(i_m)}\tilde{\sigma}_1(0). \tag{19}$$

Applying the absolute value operation yields

$$\begin{aligned}|\tilde{\sigma}_1(k)| &= \left|\frac{1}{1+4v_1^2(i_1)}\frac{1}{1+4v_1^2(i_2)}\cdots\frac{1}{1+4v_1^2(i_m)}\tilde{\sigma}_1(0)\right|\\ &\le \left|\left(\frac{1}{1+4v_{1\min}^2(i)}\right)^m\right||\tilde{\sigma}_1(0)| = \left(\frac{1}{1+4v_{1\min}^2(i)}\right)^m\\ &\quad\times|\tilde{\sigma}_1(0)|.\end{aligned} \tag{20}$$

Meanwhile, according to the definition of $v_1(k)$ in (3), it is observed that m will be infinite when k is infinite. It can be obtained that

$$\begin{aligned}\lim_{k\to+\infty}|\tilde{\sigma}_1(k)| &= \lim_{m\to+\infty}\left|\frac{1}{1+4v_1^2(i_1)}\frac{1}{1+4v_1^2(i_2)}\cdots\right.\\ &\left.\frac{1}{1+4v_1^2(i_m)}\tilde{\sigma}_1(0)\right| \le \lim_{m\to+\infty}\left(\frac{1}{1+4v_{1\min}^2(i)}\right)^m|\tilde{\sigma}_1(0)|.\end{aligned} \tag{21}$$

Since $0<1/(1+4v_{1\min}^2(i))<1$, it yields

$$\lim_{k\to+\infty}|\tilde{\sigma}_1(k)| \le \lim_{m\to+\infty}\left(\frac{1}{1+4v_{1\min}^2(i)}\right)^m|\tilde{\sigma}_1(0)| = 0. \tag{22}$$

In other words, (14) can estimate the unknown parameter σ_1 with zero steady-state errors. Based on the obtained $\hat{\sigma}_1$ and the definition of σ_1 in (7), (15) also achieves zero steady-state estimation of the frequency. In that way, an adaptive FLL is established.

Furthermore, according to (11), the orthogonal signal of the grid voltage $v(k)$ is obtained by

$$\hat{v}_\perp(k) = \frac{\hat{\sigma}_1 v(k) - v_1(k)}{\sin(\hat{\omega}T_0/4)} \tag{23}$$

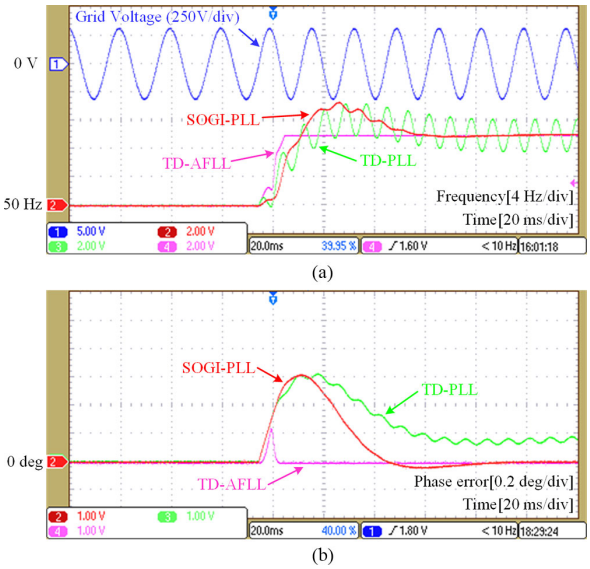

Fig. 2. Experimental results for a 10-Hz frequency jump in the grid voltage (from 50 to 60 Hz). (a) Estimated grid frequency. (b) Estimation error of the phase angle.

where $\hat{v}_\perp(k)$ is the estimated orthogonal signal of the grid voltage. The amplitude and phase angle can be obtained as

$$\hat{\mathrm{V}}(k) = \sqrt{v^2(k)+\hat{v}_\perp^2(k)} \tag{24}$$

$$\hat{\psi}(k) = \arctan\frac{v(k)}{\hat{v}_\perp(k)}. \tag{25}$$

In summary, the frequency, amplitude, and phase angle of the grid voltage can be accurately estimated by the proposed TD-AFLL, following (14), (15), and (23)–(25).

IV. Experimental Results

In this section, the performance of the proposed TD-AFLL has been evaluated by experiments under several abnormal grid conditions. For comparison, the conventional TD-PLL and SOGI-PLL are also implemented and tested. The parameters of SOGI-PLL are chosen as $k=1.414$, $k_p=92$, and $k_i=4232$. The sampling frequency is fixed at 10 kHz. Various cases are tested, and the algorithms are implemented in a dSPACE system. The grid voltage is generated by a programmable power supply.

Fig. 2 shows the experimental results for a 10-Hz frequency jump in the grid voltage (from 50 to 60 Hz). It can be observed that the proposed TD-AFLL has fast dynamics and small overshoots, compared with the other two PLLs. It takes less than one cycle of the nominal period to reach the steady state with zero steady-state errors and no double-frequency ripples. However, the TD-PLL presents a double-frequency variation, while the SOGI-PLL has relatively slower dynamics and higher overshoots.

Fig. 3 shows the experimental results under grid harmonic disturbances (0.05 p.u. for the fifth- and 0.01 p.u. for the seventh-harmonics are present in the grid voltage) and frequency jump (from 50 to 55 Hz). Observations in Fig. 3 indicate that the proposed TD-AFLL has a fast dynamic response and small

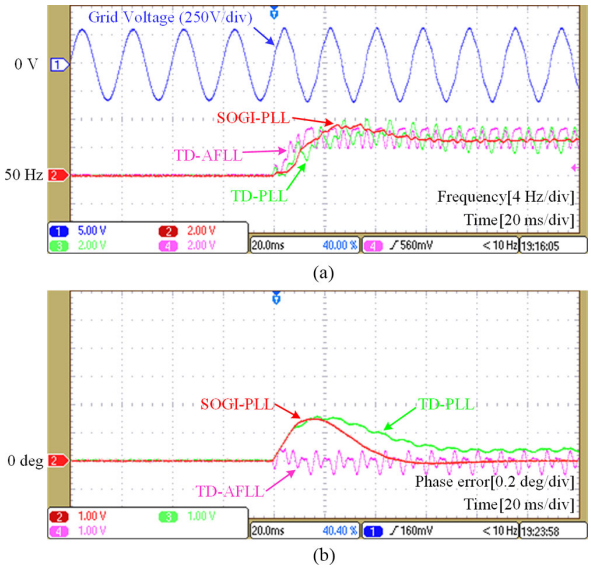

Fig. 3. Experimental results under grid harmonic disturbances (0.05 p.u. for the fifth- and 0.01 p.u. for the seventh-harmonics) and frequency jump (from 50 to 55 Hz). (a) Estimated grid frequency. (b) Estimation error of the phase angle.

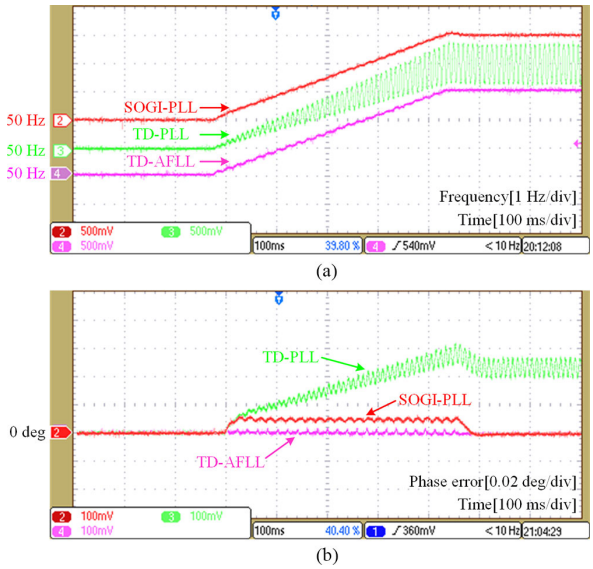

Fig. 5. Experimental results when the grid voltage undergoes a ramp-up change from 50 to 53 Hz. (a) Estimated grid frequency. (b) Estimation error of the phase angle.

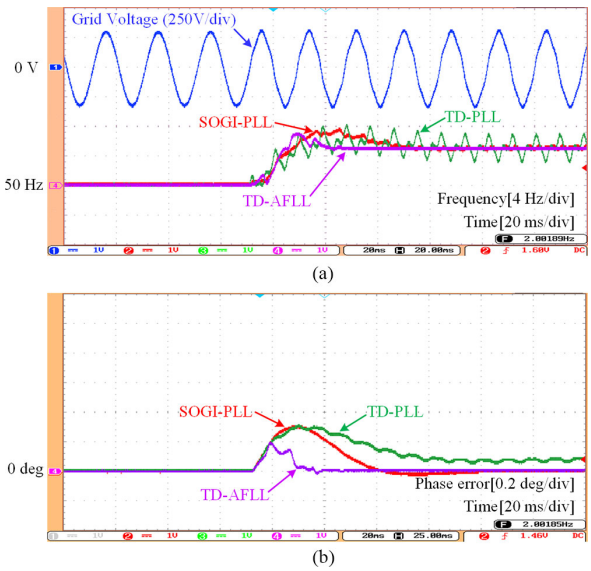

Fig. 4. Experimental results of the proposed TD-AFLL with an observer-based filter under grid harmonic disturbances (0.05 p.u. for the fifth-order and 0.01 p.u. for the seventh-order harmonics) and frequency jump (from 50 to 55 Hz). (a) Estimated grid frequency. (b) Estimation error of the phase angle.

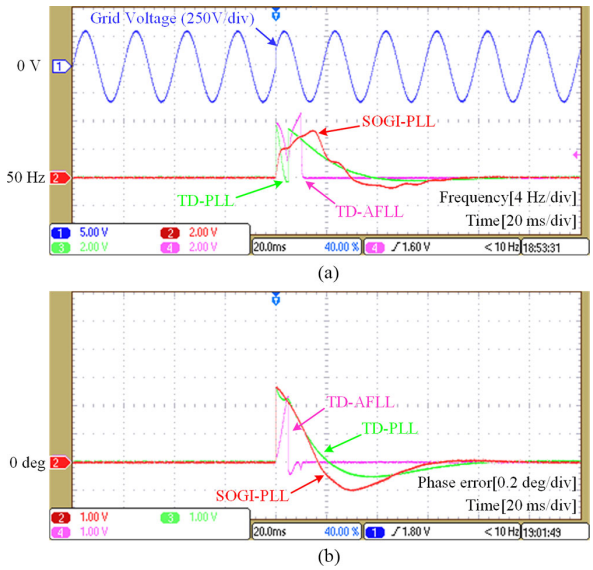

Fig. 6. Experimental results under a π/6-phase angle jump. (a) Estimated grid frequency. (b) Estimation error of the phase angle.

overshoot. Compared to the conventional TD-PLL, it removes the phase-offset error in the phase angle estimation. However, in terms of harmonic immunity, the SOGI-PLL is the best among the benchmarked methods. This is because of the high filtering characteristics of the SOGI used in this PLL, which also lead to slow dynamics to a certain extent.

In order to improve the harmonic rejection capability of the proposed TD-AFLL, additional filters can be adopted. For example, an observer-based filter [12] (detailed in the Appendix) is added before the TD-AFLL and the experimental results are shown in Fig. 4. Here, the grid voltage with harmonics and frequency jump is the same as the case in Fig. 3. It is observed in Fig. 4 that the harmonic rejection capability of the proposed TD-AFLL is improved with the observer-based filter, thus consolidating the estimation of the frequency and phase angle. Compared with the SOGI-PLL and TD-PLL, the proposed with the filter has the fastest dynamics.

Fig. 5 shows the experimental results when the grid voltage frequency undergoes a ramp-up change from 50 to 53 Hz. This case is designed to demonstrate the performance of the synchronization algorithms under frequency drifts. Nevertheless, it is seen in Fig. 5 that the proposed TD-AFLL can track the frequency change with zero phase-offset errors during the entire period, and it achieves zero steady-state errors.

Fig. 6 shows the experimental results when a π/ 6-phase angle jump occurs. It is observed in Fig. 6 that the TD-AFLL can estimate the frequency and phase angle with zero steady-state

errors. Compared with the two PLLs, the fastest dynamics by the proposed method are further confirmed.

In addition, the execution time of the TD-PLL, SOGI-PLL, and TD-AFLL is 0.96, 2.11, and 1.97 μs, respectively. It demonstrates that the conventional TD-PLL has the least computation burden.

V. Conclusion

Different from the common TD-based grid synchronization methods (usually, PLL-based), this letter proposed an adaptive FLL with fixed-length transfer delay blocks (TD-AFLL) to estimate the grid voltage parameters, including the frequency, amplitude, and phase angle. Additionally, a mathematic model was established to describe the linear relationship between the grid voltage and its transfer delay signals, and then the TD-AFLL was proposed to estimate the grid voltage parameters with zero steady-state errors. Various cases (i.e., frequency jump, harmonics, frequency ramp-up, and phase angle jump) have been tested with the proposed TD-AFLL, which has demonstrated the effectiveness in terms of fast dynamics and relatively high accuracy. Notably, the harmonic immunity of the TD-AFLL is poor, and it can be enhanced by adding filters, as exemplified in this letter.

Appendix

The added observer-based filter is

$$\dot{\hat{x}} = A\hat{x} + L\left(C\hat{x} - v\right)$$
$$v_{filter} = \hat{x}_1 \tag{A.1}$$

where v is the grid voltage, v_{filter} is the filtered grid voltage that is the input of the TD-AFLL, the state variable $\hat{x} = [\hat{x}_1, \ldots, \hat{x}_6]^T$, the matrixes $C = [\,1, 0, 1, 0, 1, 0]$, and

$$A = \begin{bmatrix} 0 & \hat{\omega} & 0 & 0 & 0 & 0 \\ -\hat{\omega} & 0 & 0 & 0 & 0 & 0 \\ 0 & 0 & 0 & 5\hat{\omega} & 0 & 0 \\ 0 & 0 & -5\hat{\omega} & 0 & 0 & 0 \\ 0 & 0 & 0 & 0 & 0 & 7\hat{\omega} \\ 0 & 0 & 0 & 0 & -7\hat{\omega} & 0 \end{bmatrix} \tag{A.2}$$

with $\hat{\omega}$ being the estimated frequency, and the filter parameter $\boldsymbol{L}$ is designed in a way that the poles of the matrix $\boldsymbol{A} + \boldsymbol{LC}$ are set as $-1.8\omega_r \pm 1.8j\omega_r, -2\omega_r \pm 2j\omega_r,$ and $-2.2\omega_r \pm 2.2j\omega_r$ with $\omega_r = 100\pi$ rad/s.

References

[1] F. Blaabjerg, R. Teodorescu, M. Liserre, and A. V. Timbus, "Overview of control and grid synchronization for distributed power generation systems," *IEEE Trans. Ind. Electron.*, vol. 53, no. 5, pp. 1398–1409, Oct. 2006.

[2] P. Kanjiya, V. Khadkikar, and M. S. El Moursi, "Obtaining performance of type-3 phase-locked loop without compromising the benefits of type-2 control system," *IEEE Trans. Power Electron.*, vol. 33, no. 2, pp. 1788–1796, Feb. 2018.

[3] Y. Lu, G. Xiao, X. Wang, and F. Blaabjerg, "Grid synchronization with selective harmonic detection based on generalized delayed signal superposition," *IEEE Trans. Power Electron.*, vol. 33, no. 5, pp. 3938–3949, May 2018.

[4] S. Golestan, J. M. Guerrero, and J. C. Vasquez, "A robust and fast synchronization technique for adverse grid conditions," *IEEE Trans. Ind. Electron.*, vol. 54, no. 4, pp. 3188–3194, Apr. 2017.

[5] S. Golestan, J. M. Guerrero, and J. C. Vasquez, "Single-phase PLLs: A review of recent advances," *IEEE Trans. Power Electron.*, vol. 32, no. 12, pp. 9013–9030, Dec. 2017.

[6] S. Golestan, J. M. Guerrero, A. Abusorrah, M. M. Al-Hindawi, and Y. Al-Turki, "An adaptive quadrature signal generation-based single-phase phase-locked loop for grid-connected applications," *IEEE Trans. Ind. Electron.*, vol. 64, no. 4, pp. 2848–2854, Apr. 2017.

[7] S. B. Kjær, "Design and control of an inverter for photovoltaic applications," Ph.D. dissertation, Inst. Energy Technol., Aalborg Univ., Aalborg, Denmark, 2005.

[8] M. Ciobotaru and F. Blaabjerg, "Improved PLL structures for single-phase grid inverters," in *Proc. Power Electron. Intell. Control Energy Convers. Conf.*, Warsaw, Poland, 2005, pp. 1–6.

[9] Y. Yang, K. Zhou, H. Wang, F. Blaabjerg, D. Wang, and B. Zhang, "Frequency adaptive selective harmonic control for grid-connected inverters," *IEEE Trans. Power Electron.*, vol. 30, no. 7, pp. 3912–3924, Jul. 2015.

[10] P. Rodríguez, A. Luna, I. Candela, R. Mujal, R. Teodorescu, and F. Blaabjerg, "Multiresonant frequency-locked loop for grid synchronization of power converters under distorted grid conditions," *IEEE Trans. Ind. Electron.*, vol. 58, no. 1, pp. 127–138, Jan. 2011.

[11] H. Yi, X. Wang, F. Blaabjerg, and F. Zhuo, "Impedance analysis of SOGI-FLL-based grid synchronization," *IEEE Trans. Power Electron.*, vol. 32, no. 10, pp. 7409–7413, Oct. 2017.

[12] W. J. Rugh, *Linear System Theory*, 2nd ed. Upper Saddle River, NJ, USA: Prentice-Hall, 1996.